



Journal Article

Efficient and Versatile Locomotion With Highly Compliant Legs

Author(s):

Hutter, Marco; Remy, C.David; Hoepflinger, Mark A.; Siegwart, Roland Y.

Publication Date:

2013-04

Permanent Link:

<https://doi.org/10.3929/ethz-a-010184788> →

Originally published in:

IEEE/ASME Transactions on Mechatronics 18(2), <http://doi.org/10.1109/TMECH.2012.2222430> →

Rights / License:

[In Copyright - Non-Commercial Use Permitted](#) →

This page was generated automatically upon download from the [ETH Zurich Research Collection](#). For more information please consult the [Terms of use](#).

Efficient and Versatile Locomotion with Highly Compliant Legs

Marco Hutter, C. David Remy, Mark. A. Hoepflinger, and Roland Siegwart, *Fellow, IEEE*

Abstract—Drawing inspiration from nature, this paper introduces and compares two compliant robotic legs that are able to perform precise joint torque & position control, enable passive adaption to the environment, and allow for the exploitation of natural dynamic motions. We report in detail on the design and control of both prototypes and elaborate specifically on the problem of precise foot placement during flight without the sacrifice of efficient energy storage during stance. This is achieved through an integrated design and control approach that incorporates Series Elastic Actuation, Series Damping Actuation, and active damping through torque control. The two legs are employed in efficient hopping/running motions for which they achieve performance similar to humans or animals. The paper is concluded by a comparison of the various design choices with respect to performance and applicability, as well as an outlook on the usage of these legs in a fully actuated quadruped.

Index Terms—Legged Robot, Torque control, Series Elastic Actuation, ScarlETH

I. INTRODUCTION

ANIMALS and humans can exhibit astonishing levels of *versatility* when moving in rough and highly unstructured terrain, while, at the same time, they are able to locomote with high *speed* and great *efficiency* on less demanding surfaces. We can easily climb over obstacles the size of our leg length, or move along steep slopes by carefully selecting footholds and precisely moving our limbs to keep balance at all times. On flat terrain, however, we switch to periodic gaits (such as walking or running) which are largely driven by the natural dynamics of our mechanical structure [1] [2] and are hence energetically efficient.

Over the past decades, the robotics community was able to successfully reduce the performance gap between robots and nature in terms of *versatility* by building on their strong background in industrial robotics. The resulting systems (often highly sophisticated humanoid robots with a large amount of DoFs [3] [4]) are built mechanically rigid and are driven by stiff actuators with large gearbox transmissions and high-gain controllers. This design allows them to precisely follow kinematic joint trajectories, thus enabling a large variety of motion tasks. Similar systems with more than two legs were developed for static locomotion in rough terrain [5] and are able to transverse all kinds of obstacles. A recent example of

M. Hutter, M.A.H. Hoepflinger, and R. Siegwart are with the Autonomous Systems Lab, Swiss Federal Institute of Technology (ETHZ), Zurich, Switzerland (mahutter@ethz.ch). C. D. Remy is with the Dep. of Mech. Engineering, University of Michigan, Ann Arbor, MI (cdremy@umich.edu)

Manuscript received Oct. 31, 2011, revised Apr. 11, 2012, accepted Sep. 16, 2012.. This work was supported in part by the Swiss National Science Foundation (SNF) (project 200021_119965/1), the Swiss National Centre of Competence in Research (NCCR), and the Hans-Eggenberger-Foundation.

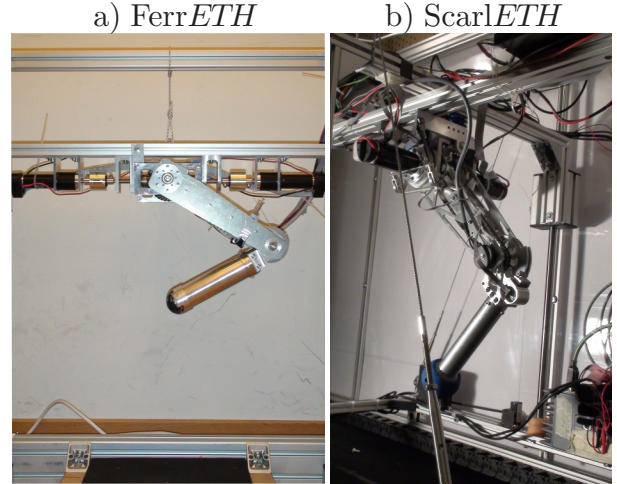


Fig. 1. Two compliant legged prototypes developed to investigate versatile and efficient locomotion. Shown are in (a) FerrETH (First Elastic Running Robot) and in (b) ScarlETH (Series Compliant Articulated Robotic Leg).

research in this direction is the DARPA Learning Locomotion Challenge (e.g., [6] [7]), in which several groups pushed the state of the art with respect to motion planning and execution in unstructured, yet fully known terrain. Towards the same direction, our group developed ALoF; a highly mobile quadruped [8] which is employed to study the usage of haptic feedback to estimate surface properties [9].

In stark contrast to this kinematic approach are robots that exploit their natural dynamics to improve locomotion *speed* and *efficiency*. Initiated by Mark Raibert's seminal work on hopping robots with pneumatic pistons [10], researchers started to use elastic elements to temporarily store kinetic energy and thus preserve it throughout the gait cycle. This makes locomotion efficient and enables running at high speeds. Conceptually, such robots reflect the abstract model of the spring loaded inverted pendulum (SLIP [11] [12]) that is often used to explain the energetics of running motions found in nature. Depending on the particular design, springs are integrated directly in prismatic legs [13] [14] [15] or into the knee and ankle joints of articulated designs [16] [17] [18] [19] [20]. In all these robots, motion emerges to a large extent passively from the mechanical dynamics and actuators are merely used to compensate for friction and impact losses.

So far, all presented systems share one substantial drawback: They either solve the *versatility* OR the *efficiency* problem, but never both. Kinematically controlled robots must create the entire motion actively, which tends to make them quite inefficient. Additionally, they cannot tolerate high impact

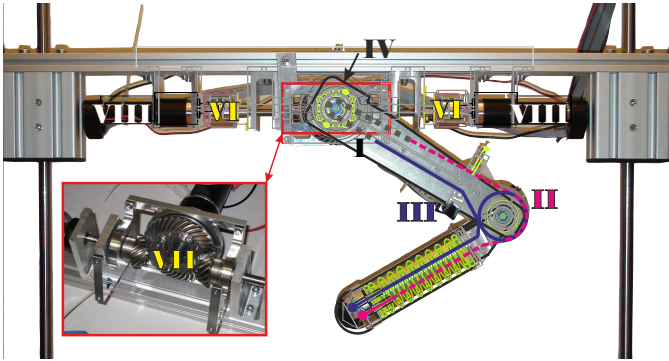


Fig. 2. FerrETH is driven by a differential gearbox in combination with SDA actuators at the hip joint and a high compliant SEA in the knee.

forces and are thus unsuited for highly dynamic maneuvers. And since they are unable to adapt passively to uncertainties in the environment, they require extensive (and expensive) sensor equipment to cope with unforeseen situations. Robots that exploit natural dynamics are, on the other hand, inherently hard to control and are thus gravely limited with respect to their application. Many of the existing solutions are unable to turn or stop [21], and to the best of our knowledge, solutions for robotic devices that demonstrate both, precise kinematic control as well as the exploitation of natural dynamics, are still not available.

As a step towards closing this gap, our group developed a series of compliant, highly integrated legs (Fig. 1) that allow for precise joint torque and position control, enable passive adaption, and allow for natural dynamic motions. In this paper, we introduce, discuss, and compare two of these legs, FerrETH (First Elastic Running Robot) and ScarlETH (Series Compliant Articulated Robotic Leg). We largely extend findings of previous studies with FerrETH [22], [23] and ScarlETH [24], [25] and compare them in terms of performance and applicability. We further report in detail on their design and control and elaborate specifically on how to create the necessary damping without sacrificing efficiency.

II. SYSTEM DESIGN

Design guidelines for legged systems that are specifically built for dynamic maneuvers can be directly adopted from their counterparts in nature. For example, to reduce the leg inertia (to allow faster joint motion and decrease losses at touchdown) segments should be built as lightweight as possible and heavy components, such as actuators, should be placed close to the main body. Elastic elements should decouple actuators and joints in order to make the system robust against impact collisions, to allow passive adaptation, and to enable the temporary storage of energy [11]. To maximize mobility, one should aim for a large range of motion in all joints and thus tightly integrate all mechanical and electrical components. In this Section we will show how these design guidelines have been implemented in two different leg prototypes while focusing specifically on different actuation solutions based on Series Elastic (SEA) and/or Series Damping (SDA) Actuation. A comparison of the mechanical properties and components of both legs can be found in Table I.

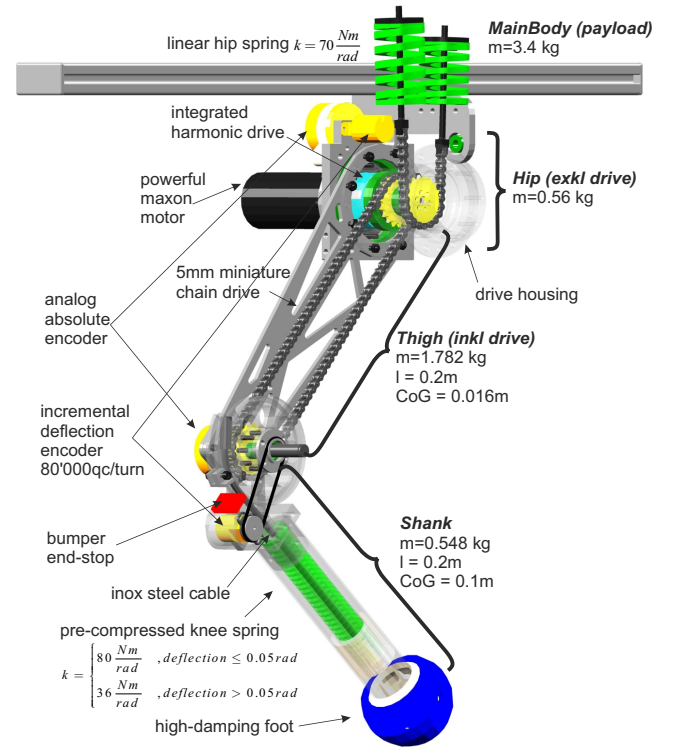


Fig. 3. Detailed system description of ScarlETH including a visualization of the SEA principle for hip and knee flexion/extension.

A. FerrETH

To compactly integrate the hip (*Maxon RE-25 20 W DC motors with Maxon GP-32 1:51 planetary gearbox*) and knee actuators (*Maxon RE-35 90 W DC motors with Maxon GP-42 1:26 planetary gearbox*) within the main body of FerrETH (Fig. 2), a differential drive (VII) couples the degrees of freedom for hip abduction and adduction (c.f., [8]). Additionally, the knee motor (IV) is integrated in a hollow shaft going through the bevel gear for hip flexion/extension and from there connected through a miniature chain-drive (I) and two cable-pulleys (II,III) to a highly compliant spring (V, $12 \text{ Nm}/\text{rad}$) placed in the shank. This spring creates a large compliance in the knee joint and allows for temporary energy storage during ground contact. It dominates the natural dynamics of the entire leg. The passive deflection of this spring is measured using a high resolution incremental encoder in the knee (*AVAGO AEDA3300 optical incremental encoder with 80'000 q/turn*). Absolute potentiometers (*Contelec Wal300*) are used to initialize the motor encoders on the remaining axes.

During running, most of the energy is being stored in the knee joint which hence undergoes substantial passive deflections. The hip actuators, on the other hand, are primarily used for precise foot positioning during the flight phase, and do not store any energy. High performance elastomer-bushings (VI) are thus mounted in series with the hip motors (VIII) and form a SDA that protects the gearbox from impacts while passively suppressing undesired joint deflections.

The overall design benefits from the fact that both hip motors can be rigidly attached to the main body and that the knee motor is positioned very close to the center of rotation of

TABLE I
KEY DATA OF FERRETH AND SCARLETH

parameter	FerrETH	ScarETH
mechanics		
m_S (Shank)	0.43 kg	0.42 kg
m_T (Thigh)	1.7 kg	1.56 kg
m_H (Hip)	1.9 kg	0.56 kg
$m_{Payload}$	0 kg	3.0 kg
θ_S	1.2E-3 kNm^2	3.5E-3 kNm^2
θ_T	7.8E-3 kNm^2	8.5E-3 kNm^2
l_S	0.18 m	0.2 m
l_T	0.2 m	0.2 m
s_S^a	0.074 m	0.08 m
s_T^a	0.005 m	0.016 m
actuation		
hip motors	Maxon DC RE25 (20W)	Maxon DC RE35, 90W
knee motor	Maxon DC RE35 (90W)	Maxon DC RE35, 90W
hip gearbox	Maxon GP32 ^b (1:51)	HDC ^c (1:80)
hip transmission	differential (1:2.5)	direct (1:1)
knee gearbox	Maxon GP42 ^b (1:26)	HDC ^c (1:80)
knee transmission	cable pulley ^d (1:3.3)	chain (17:19)
hip stiffness	nonlinear > 100 Nm/rad	70 Nm/rad
knee stiffness	12 Nm/rad	36 Nm/rad
sensors		
spring deflection	AVAGO AEDA3300 (80'000 qc/turn)	
abs. joint position	Contelec WAL300 Potentiometer	

^adistance CoG to predecessor joint^bMaxon Planetary Gearbox^cHarmonic Drive CSG^dkevlar rope

the hip joint. This simplifies cabling to a large extent, allows for a better protection of all actuators, centralizes the mass near the main body, and achieves a large range of motion. Hip adduction/abduction range is $+90/-45^\circ$, hip flexion/extension $\pm 75^\circ$, and knee flexion/extension $+20/-170^\circ$ from the vertical configuration. From a mechanical point of view, the main drawback of this design is the additional weight of the massive differential drive and the undesired play in the bevel gears and the planetary gearboxes of the motors.

B. ScarETH

To avoid coupling effects and reduce the overall weight, the differential drive concept is not repeated in ScarETH (Fig. 3). To keep the leg inertia small, a single, weight optimized drive unit containing harmonic drive gearboxes and two *Maxon RE35* 90 W DC motors for hip and knee flexion/extension serves as the hip joint axis. Improved from the previous design, a more robust chain drive and steel cable pulley connect the knee motor to a large compression spring in the shank. The same absolute potentiometers and incremental deflection encoders as in FerrETH are used in all joints to give precise state measurements at all time.

A major design difference in comparison to the FerrETH leg is the actuation of the hip joints. Instead of very stiff and highly damped elastomers, steel springs are used for series elastic actuation. Since they show nearly no passive damping, this design choice entails a fundamental shift from position/velocity control on joint level to a fully torque controlled approach. This requires adequate sensing technologies and a completely backlash free design with pre-compressed joint springs and harmonic drive gearboxes.

This design has additional advantages: due to the high integration, a high power to weight ratio is achieved for the

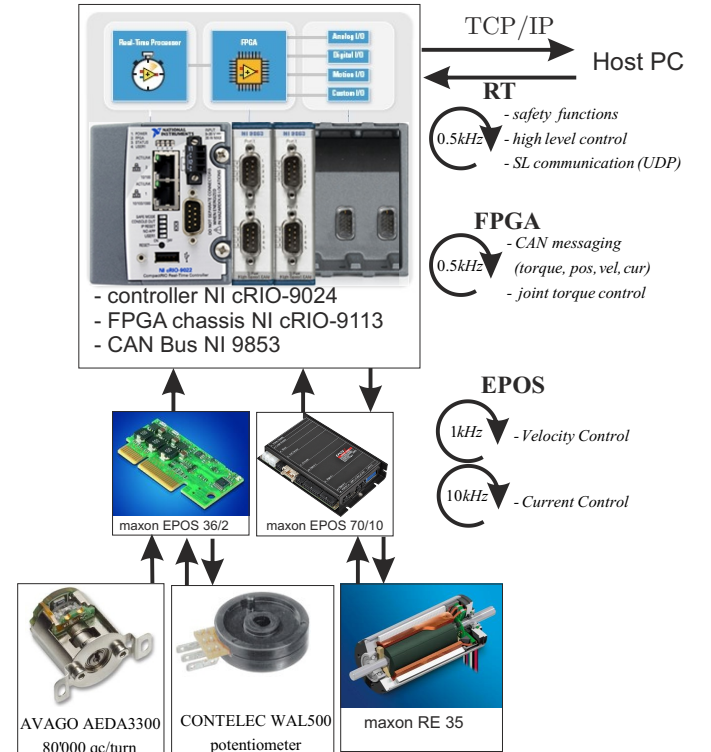


Fig. 4. The electronic control setup for FerrETH and ScarETH is based on a NI compactRIO (RT) in combination with *Maxon* EPOS motor controllers.

overall robot. The compact design with the chain and cable pulley transmission results in large mobility for all joints. The leg can be completely extended and retracted (knee joint $[-175^\circ, +60^\circ]$) while the hip joint can undergo a swing angle of $[-80^\circ, +80^\circ]$. Perfect linearity in the joint springs and very high resolution encoders give very accurate joint torque measurements and allow for high fidelity force control.

C. Electronic Setup

Both legs use the same electronic setup for control, as shown schematically in Fig. 4. Position, torque, and high level control are implemented on a *National Instruments compactRIO* (a realtime system combined with an FPGA), which is connected via CAN bus to a number of *Maxon EPOS*-modules. They are used as sensor boards to read out the encoder values and for motor control running the low level control loops for velocity and current regulation. Due to payload restrictions, these control electronics are stored off-board in the FerrETH platform.

III. ELASTIC ACTUATOR DESIGN

The goals of versatility, speed, and efficiency seem to be contradictory when it comes to actuation and control [21]. To make a hopping or running motion efficient, the mechanical damping of the elasticities in the system needs to be kept as small as possible to allow efficient energy storage when the leg is loaded during stance. However, low-damped elasticities can create undesired deflections and oscillations that make fast and precise foot positioning very difficult when the leg is unloaded

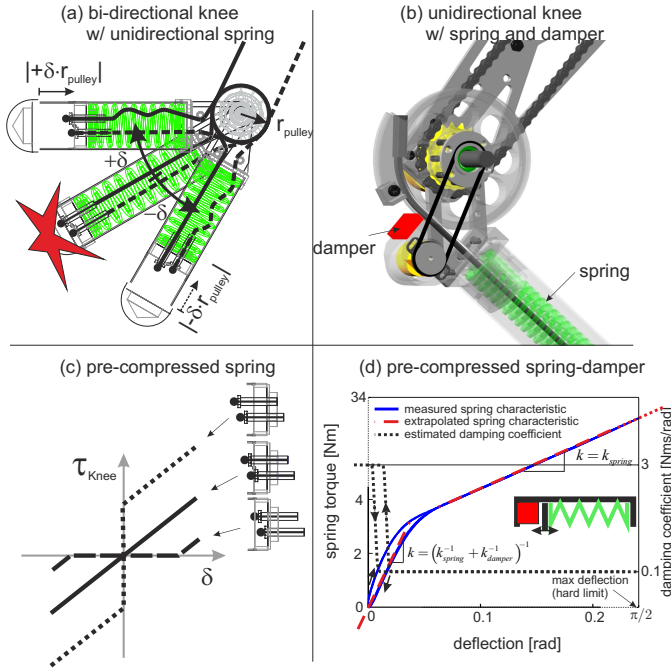


Fig. 5. The knee actuator of FerrETH exploits internal collisions (a) to increase damping during flight that can be adjusted through variable spring pre-compression (c). ScarlETH benefits from a non-linear spring-damper characteristic (b,d) that shows minimal damping and a linear, hysteresis-free torque-deflection ratio during stance (efficiency) and maximal damping with hysteresis due to the spring-damper pre-compression during flight phase (versatility).

during flight. This "damping dilemma" (high damping and no oscillations during flight, low damping and efficient energy storage during stance [22]) requires novel solutions based on hand-in-hand integration of *hardware* and *controller* design. In this sections, different concepts based on internal collisions, nonlinear damping, and active damping are presented and compared.

A. Knee Actuation

For the two systems, the oscillation frequencies of the unloaded shank segment (i.e., during flight) can be computed as:

$$f = \frac{1}{2\pi} \sqrt{\frac{k}{m_S s_S^2 + \theta_S}} = \begin{cases} 10\text{Hz} & (\text{FerrETH}) \\ 12\text{Hz} & (\text{ScarlETH}) \end{cases} \quad (1)$$

With these high eigenfrequencies, damping of the knee oscillations (during the flight phase) is very difficult to achieve through control alone. Consequently, methods for passive mechanical damping during the flight phase need to be employed. In our lightweight design it is impossible to use additional couplings, brakes, magnetorheological systems, or other adjustable dampers [26]. Instead, we take advantage of the fact that the leg is always loaded during the stance phase and that this loading only happens in one direction.

In FerrETH, damping of the unloaded leg is achieved through internal dynamic effects of the spring. Every time, the knee is crossing the neutral position (Fig. 5a), the direction of motion of the uni-directional spring must change. This results

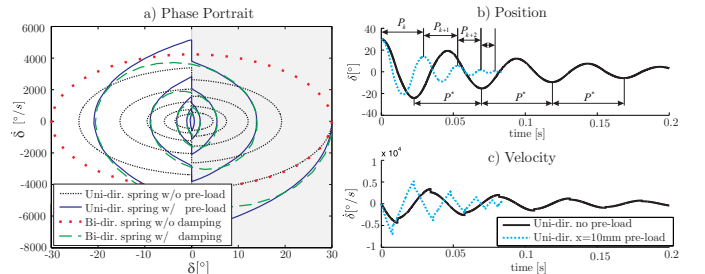


Fig. 6. Internal collisions in the knee SEA of FerrETH cause higher damping through impact losses (a) as well as a phase shortening (b).

in an internal mechanical collision within the spring, energy is lost, and the motion is slowed down. Since this only happens when the knee is unloaded, energy storage during stance is unaffected by this process. In [22] we identified two effects that contribute to increased damping during flight phase.

First, the internal collisions lead to an instantaneous reduction in joint deflection speed $\dot{\delta}$ ($-$ = before collision, $+$ = after collision), which can be expressed as a function of the total shank inertia $\bar{\theta}_S = \theta_S + m_S s_S^2 + m_F s_F^2$, the spring mass m_F , the corresponding joint distance s_F , and the pulley radius r according to:

$$\frac{\dot{\delta}^+}{\dot{\delta}^-} = \frac{\bar{\theta}_S - m_F r^2}{\bar{\theta}_S + m_F r^2} = \epsilon \quad (2)$$

In a full period, the spring undergoes two collisions in the forward and backward motion. The speed over a full cycle hence scales with $\frac{\dot{\delta}_{k+1}}{\dot{\delta}_k} = \epsilon^2$. Neglecting all other energy losses in the spring (e.g., due to viscous damping or friction), this leads to a kinetic energy (T) loss that is directly related to a decrease of the deflection amplitude $\hat{\delta}$ (Fig. 6a):

$$\frac{T_{k+1}}{T_k} = \frac{\frac{1}{2}\bar{\theta}_S \dot{\delta}_{k+1}^2}{\frac{1}{2}\bar{\theta}_S \dot{\delta}_k^2} = \frac{\frac{1}{2}cr^2 \hat{\delta}_{k+1}^2 + c\bar{x}_p r \hat{\delta}_{k+1}}{\frac{1}{2}cr^2 \hat{\delta}_k^2 + c\bar{x}_p r \hat{\delta}_k} = \epsilon^4 \quad (3)$$

This means, the damping ratio $\frac{\dot{\delta}_{k+1}}{\dot{\delta}_k}$ can be adjusted within the range of ϵ^4 and ϵ^2 as a function of the spring pre-compression \bar{x}_p and the spring stiffness c .

Second, the oscillation period P is shortened by an increased pre-compression \bar{x}_p (Fig. 5c) of the spring (Fig. 6b). This can be expressed as

$$\frac{P_{k+1}}{P_k} = \frac{\pi - 2\arcsin(\bar{x}_p / (\bar{x}_p + r\hat{\delta}_{k+1}))}{\pi - 2\arcsin(\bar{x}_p / (\bar{x}_p + r\hat{\delta}_k))}, \quad (4)$$

and additionally reduces the time until an initial deflection vanishes.

In ScarlETH a different strategy is used that takes advantage of the fact that the knee joint during the stance phase is always loaded in the same direction [25]. We apply a combination of SEA and SDA (Fig. 5b) to prevent oscillations during flight while keeping damping low during stance. In this design, a steel spring is pre-compressed against a damper unit, which creates an overall nonlinear spring-damping characteristic (as shown in Fig. 5d). If the leg is in contact with the ground, the actuator is continuously operating in the linear, low

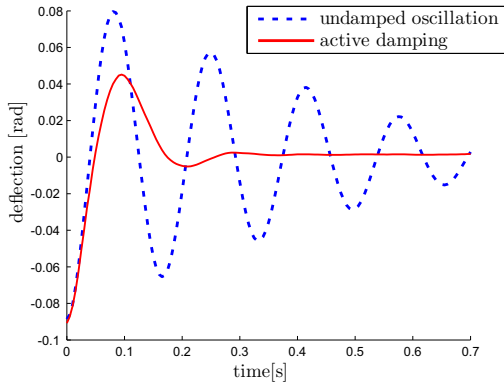


Fig. 7. Experimental results of active damping in the antagonistically precompressed hip joint of StarlETH demonstrate a highly improved behavior during flight phase.

damped region of the spring (SEA), allowing for efficient energy storage. During flight phase, the knee joint operates in the high-damping and high stiffness region (SDA) such that undesired deflections are immediately suppressed. In this region, additional hysteresis effects further improve position control while degrading the torque controllability. The latter is no problem, since the SEA/SDA is only operated in this region during flight phase.

B. Hip Actuation

The SDA actuation in the hip joint of FerrETH reduces the joint position control to a simple problem of motor position control. The high stiffness and strong damping in the elastomers quickly suppress any undesired deflections. The hip actuation concept of ScarlETH, on the other hand, is fundamentally different. Instead of relying on passive mechanical damping, the hip joint is designed in a way that active damping can be achieved through force control. This requires a careful selection of the spring stiffness. Springs that are too stiff let the joint oscillate at frequencies that are impossible to control with the limited bandwidth of the actuators, while springs that are too compliant require large travel in the actuators to produce a desired force. This would decrease the force control bandwidth and drastically reduce performance.

With the chosen stiffness value (see Table I), the eigenfrequency of the hip joint motion evaluates to

$$f = \frac{1}{2\pi} \sqrt{\frac{k_{Hip}}{\theta_T + m_T s_T^2 + \theta_S + m_S (l_T + s_S)^2}} = 6.25 \text{ Hz}, \quad (5)$$

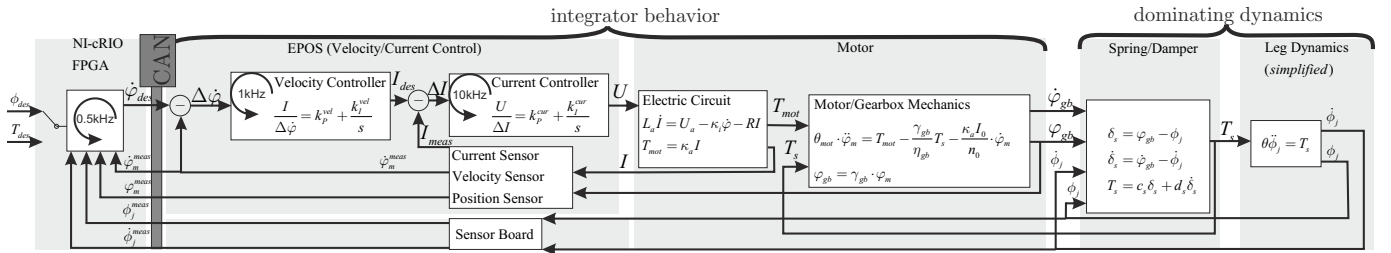


Fig. 8. The control structure is built in a cascaded structure with position/torque control implemented on the NI compactRIO device and a velocity controlled motor. The mass-spring dynamics of the leg are dominating (all other loops are much faster), allowing for large simplifications for theoretical control design.

which can be actively damped with the hip actuator. Both, the eigenfrequency of 6.25 Hz, as well as the active damping performance are shown as experimental results in Fig. 7. For these plots, the hip joint was deflected by an external force and released while the joint position was recorded using the incremental joint encoder. The controller design is discussed in more detail in Section IV-A.

IV. LOCOMOTION CONTROL

The different joint designs presented in the previous section allow for a large variety of applications, yet they pose fundamentally different challenges in terms of control. In this section, we will focus on these challenges, present different approaches for joint position, torque, and efficient motion control, and show their applications in 1D hopping and 2D running. Independent of the chosen control strategy, the motors are always considered as velocity sources. A fast, low level velocity and current controller compensates for gearbox friction and inertia effects and regulates the motor velocity. Joint position or torque control, as well as high level running/hopping coordination are then implemented in a cascaded structure as it is depicted in Fig. 8.

A. Position Control

High damping (FerrETH, hip), internal collisions (FerrETH, knee), and nonlinear spring-damper characteristics (ScarlETH, knee) reduce the position control problem of these joints to a trivial problem of motor position control. In contrast to that, active damping is required in the hip joint of ScarlETH since such a motor position controller implementation leads to natural joint oscillations. They are marked with a black circle in the pole-zero map of Fig. 9. The dominating and well known spring-mass-damper dynamics expressed as a function of the motor angle φ_m , joint angle ϕ_j , stiffness c and damping d

$$\theta \ddot{\phi}_j = c(\varphi_m - \phi_j) + d(\dot{\varphi}_m - \dot{\phi}_j) \quad (6)$$

in combination with the integrator behavior of the velocity controlled motor (bandwidth 100Hz [24]) allows the implementation of a LQR control structure based on joint and motor measurements (no observer required):

$$\dot{\varphi}_m = k_1(\phi_{des} - \varphi_m) - k_2(\dot{\phi}_{des} - \dot{\phi}_j) + k_3(\ddot{\phi}_{des} - \ddot{\phi}_j) \quad (7)$$

The closed loop joint position transfer function is:

$$\frac{\Phi_j(s)}{\Phi_{des}(s)} = \frac{(k_1 - k_2 + k_3 s)(c + sd)}{\theta s^2 (s + k_1) + (s + k_1 - k_2 + k_3 s)(c + sd)} \quad (8)$$

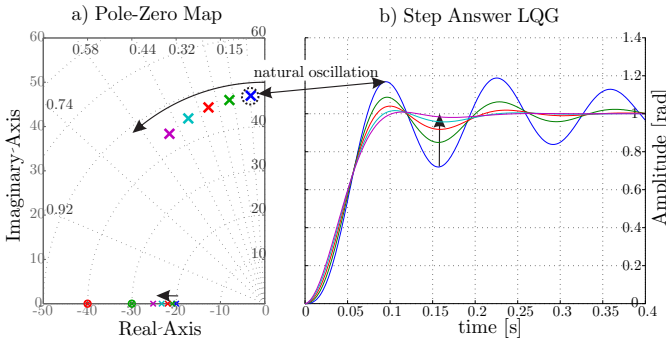


Fig. 9. A LQR based control design allows to increase damping without sacrificing speed: the oscillating poles are shifted to higher damped regions (a) which largely improves the step response (b).

Proper adjustment of the control gains $k_1 > k_2 > 0$ and $k_3 > 0$ shifts the poles to higher damped regions while keeping the response time of the system (Fig. 9).

B. Torque Control

In StarlETH, the identified spring characteristic in both the hip and knee spring shows nearly perfect linearity with no hysteresis effects. A linear, least square model fit shows that the springs can be used as a torque sensor with a linear regression coefficient of $R = 0.999$ (hip and knee) and a mean absolute error of $\overline{|e|}_{\text{hip}} = 0.08 \text{ Nm}$ and $\overline{|e|}_{\text{knee}} = 0.05 \text{ Nm}$. Hence, the integration of additional load cells that are expensive and might break under high peak loads can be avoided and the desired joint torques are achieved by actively regulating the spring deflections. Such a torque controller must be implemented with regard to two design criteria: First, fast reference tracking (high closed loop torque bandwidth in combination with high robustness) must be achieved. Fig. 10a shows the response to a desired step of 3 Nm in simulation and experiment. The system can follow the reference in about 30 ms. The closed loop transfer function (Fig. 10c, blue lines) emphasizes the drawback of high compliance: with increasing amplitudes, the bandwidth substantially drops due to saturation effects. Using the complete model with the validated control parameters, the transfer function is estimated for a set of amplitudes based on a sinusoidal input. The bandwidth varies between 28 Hz for 1 Nm (dashed), 15 Hz for 5 Nm (dash-dotted) and 11 Hz for 10 Nm (dotted). The closed loop system is robust with a phase margin of more than 85° . Consequently, the resulting bandwidth is poor compared to systems with stiffer springs, yet they are still within the range of Pratt's electrical SEAs (5-25 Hz [27]) or human assistive devices [28], and above the frequency range that is typically found in human motion (4-8Hz [29]).

Second, next to a fast reference signal response, good disturbance rejection is crucial. This can be tested for a zero torque reference with external joint disturbance (Fig. 10b). Using a PID torque controller with low integrator gains causes substantial joint deflections (black solid line) due to the phase delay between the joint and motor angles [24]. As depicted in Fig. 10c, the sensitivity of the PID controller (red dashed line) has a flat ascent (20 dB/dec) that would require higher integral

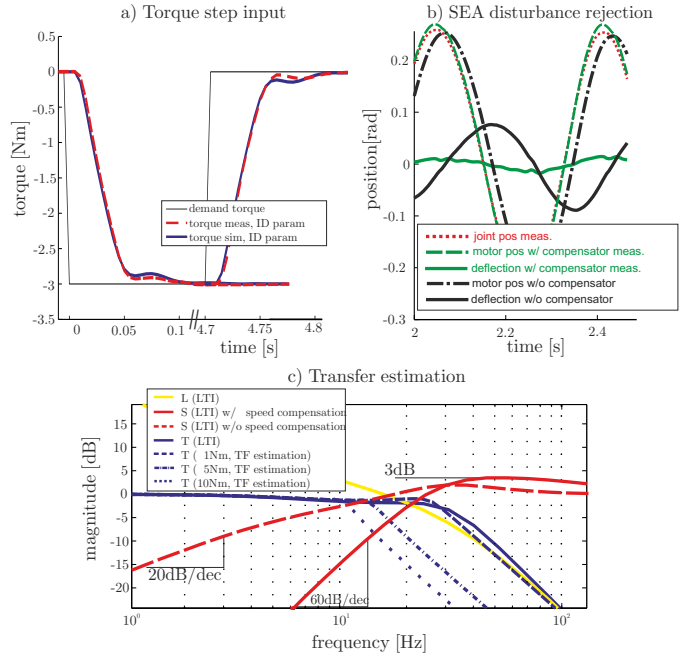


Fig. 10. Experimental and simulated results of the SEA torque controller show a fast step answer (a) with no overshoot. Using an additional disturbance compensator based on joint speed measurements allows to significantly reduce the spring deflections when externally disturbed (b). The transfer function estimation (c) shows a bandwidth of up to 28 Hz for small amplitudes; about 11 Hz remain when saturation effects occur. Due to very small integrator gains, the overshoot is kept small ($T_{\max} < 1 \text{ dB}$) and good robustness with a phase margin of more than 85° is achieved. The feedforward speed compensator allows to largely improve the sensitivity to a 60 dB/dec ascend.

gains to keep the torque ripple small [30]. Unfortunately, this degrades the reference following behavior, having a negative influence on the robustness as well as an increased overshoot. Hence, a disturbance compensator is implemented that has no influence on the properties of the closed loop controller. The low-pass behavior of the velocity controlled motor and the precise joint speed estimation (minimal discretization noise) allows to use the joint velocity input directly as a feed-forward path. This inherently ensures that the output value is independent of the input value for the stationary case since $\dot{\phi}_m(s=0) = \dot{\phi}_j(s=0)$. The sensitivity is still bounded by 3 dB but shows a much better behavior for lower frequencies (at which the system is usually operated) with a slope of 60 dB/dec (Fig. 10c, red solid line). The zero torque behavior successfully demonstrates this improved performance with highly reduced joint deflections (Fig. 10b, green solid line). At this point, the high compliance clearly helps, since the time constant for the required reaction is lower than in a system using stiff springs.

C. Exploiting Natural Dynamics

The primary goal of the presented leg designs is to allow for the exploitation of natural dynamic motions. This means excess kinetic energy should be stored in the elastic elements and recovered when needed. Actuators should avoid performing negative work and merely compensate for energy losses due to damping and impact collisions. In this context, the immediate question arises how such an efficient behavior

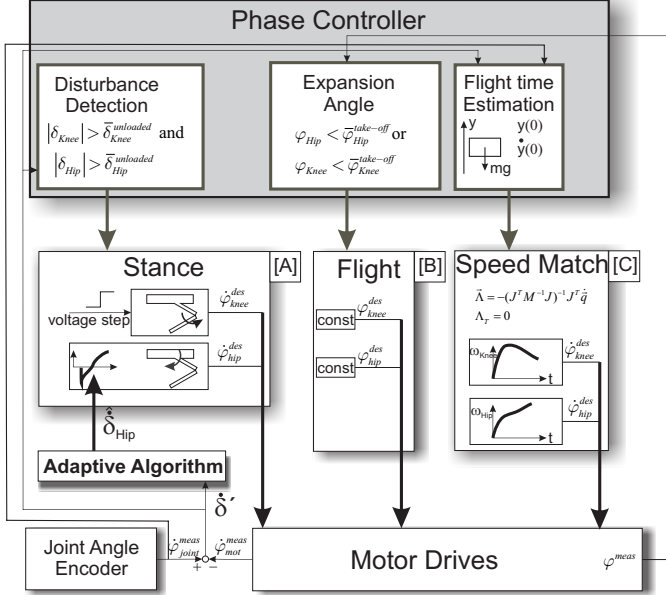


Fig. 11. A 3-pronged control algorithm [23] is implemented for online adaptation of the hip joint profiles to ensure stable hopping in place.

can be achieved in terms of control. This is not a trivial problem. Similar to animals, which employ different gaits for different running speeds, the actuator inputs for a robot that optimally exploit the natural dynamics of the system might need to change as a function of locomotion speed or other parameters [31]. One possibility to create motor trajectories that excite periodic oscillations for running motions is by using optimal control techniques [32] in simulation and transferring the results to the actual robot. However, since these methods require very accurate models of the hardware, it is difficult to directly transfer the results to an actual system. In the following, we thus want to present two more direct approaches to this problem.

1) Adaptive Trajectory Control:

In [23] we implement a 3-pronged adaptive control algorithm (Fig. 11) that takes full advantage of the presented joint design. During stance phase, the knee motor is thrust with a desired speed profile $\dot{\varphi}_{knee}^{des}(t) > 0$ to inject energy into the system. This ensures that during the stance phase, the knee motor never performs negative work. At the same time, the hip motor is controlled to ensure a purely vertical motion of the main body and to prevent slippage of the contact point. Starting from an initial analytical estimation of the joint trajectories based on simulations, the hip profile is adapted over a series of jumps to match the non-slippage constraint. In [23] it is shown that the algorithm converges within three successive steps.

2) Running based on Virtual Model Control:

An intuitive approach for the control of single legged running emerges directly from biomechanical studies showing that a complex running behavior can be described to a large extent by very simple spring-mass models [11] [12]. During flight phase, the foot point is positioned to keep balance, during stance

phase, energy is introduced to shape the running motion - an approach that was already implemented in the early Raibert hoppers at the MIT leg lab [10]. In ScarlETH, these control strategies can be applied directly:

First, highly damped position control allows fast foot positioning during flight phase. According to [10], the angle of attack is adapted as a function of the horizontal position x and speed \dot{x} while an offset angle α_0 compensates for the horizontal impacts due to the articulated design:

$$\alpha(x, \dot{x}) = k_{FF}\dot{x} + k_{FB}(k_{Pos}(x_{des} - x) - \dot{x}) + \alpha_0 \quad (9)$$

whereby $k_{FF} > 0$ corresponds to the feedforward, $k_{FB} > 0$ to the feedback, and $k_{Pos} > 0$ to the position gain.

Second, precise torque control allows the emulation of different spring-damper behaviors between the ground contact point and the CoG of the leg through a virtual force \mathbf{F}_{virt} . Based on Jacobi-transposed mapping, the desired forces in Cartesian space can be mapped into joint coordinates \mathbf{q}_j such that they create the same effect as the virtual force element [33]:

$$\mathbf{T} = \mathbf{J}^T \mathbf{F}_{virt} \quad (10)$$

$$\mathbf{J} = \frac{\partial \mathbf{r}_{Hip} - \partial \mathbf{r}_{Foot}}{\partial \mathbf{q}_j} \quad (11)$$

The SLIP behavior implies a vertical spring-damper force according to

$$F_{virt}^y = c_y(y_0 - (y_{Hip} - y_{Foot})) + d_y(-\dot{y}_{Hip}) + g_y \quad (12)$$

with the desired spring stiffness c_y , damping coefficient d_y , and gravity compensation term g_y . Due to bandwidth limitation of the actuator, the virtual stiffness (as well as the damping coefficient) is bounded by $c_y^{max} \approx \omega_{BW}^2 m_{Hip}$ (actuator bandwidth ω_{BW} and hip mass m_{Hip}). To nevertheless ensure efficient excitation, we additionally constrained the knee joint motion such that the actuator always introduces energy into the system $P_{knee} > 0$. In terms of velocity, this can be expressed as $\dot{\varphi}_m > 0$, since throughout stance the torque at the knee joint is always positive.

To control the forward running motion, the horizontal force is modulated based on a simple proportional position controller:

$$F_{virt}^x = sat(k_x(x_{des} - x_{base})) \in [-F_{neg}, F_{neg}] \quad (13)$$

To avoid tipping over or slipping, the force is limited by a saturation function $sat()$.

V. RESULTS

Both systems were tested thoroughly in 1D and 2D hopping experiments. Therefore, we constructed a test bench that consists of a planar guiding unit connected to the main body. The entire system can freely move in horizontal and vertical direction on a rolling unit with low friction. Cable pulley encoders in both directions are used to measure the absolute position of the main body. Figure 12 shows the knee joint and motor position during the stance phase of FerrETH(a) in 1D hopping based on the trajectory adaptation algorithm (Section IV-C1) respectively of ScarlETH(b) in 2D virtual

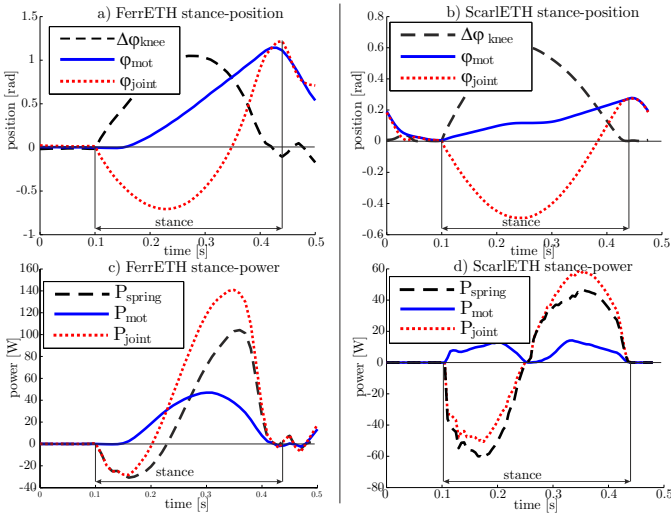


Fig. 12. The experimental results of hopping in place with FerrETH and ScarlETH indicate the benefit of the large compliance in the knee joint: (a,b) the motor travel distance (and its speed) remains only a fractional part of the joint motion. (c,d) the motor introduces energy during the entire stance phase with small peak power and zero negative work.

model hopping (Section IV-C2). As expected, the spring compliance ensures that the travel distance of the motor is much smaller than the actual joint motion. Further more, the motor is always delivering positive power (Fig. 12c,d). The spring stores kinetic energy after impact and returns it before lift-off. This is in stark contrast to a stiff actuation approach in which breaking and accelerating energy need to be provided by the actuator. To be able to compare the mechanical efficiency of energy storage in single legged hopping (among robots but also in comparison to values found for human or animal in-place hopping), we define the ratio between the positive work performed by the actuator and the positive joint work as the hopping efficiency η :

$$\eta = 1 - \frac{\int_T \max(P_{mot}, 0) dt}{\int_T \max(P_{joint}, 0) dt} \quad (14)$$

Since electric energy recuperation is generally not possible, we use the notation $\max(P, 0)$. Hence, (14) indicates how much of the positive mechanical work in a hopping cycle ($\int_T \max(P_{joint}, 0) dt$) can be provided passively. To keep the efficiency maximal, the actuator should never perform negative work. Additionally to the efficiency coefficient η , the maximal joint speed in relation to the maximal motor speed $\omega_{rel} = \frac{\dot{\phi}_{joint}}{\dot{\phi}_{mot}}$, as well as the maximal joint power in relation to the maximal motor power $P_{rel} = \frac{P_{joint}}{P_{mot}}$ clearly indicate the benefit of high compliant SEA:

	FerrETH	ScarlETH
η	0.33	0.64
ω_{rel}	3.9	4.7
P_{rel}	2.2	4.1

Both robotic devices have an excellent mechanical efficiency. Since energy can be introduced to the system throughout the entire stance phase (not only during the acceleration phase), less power is required for the same amount of work

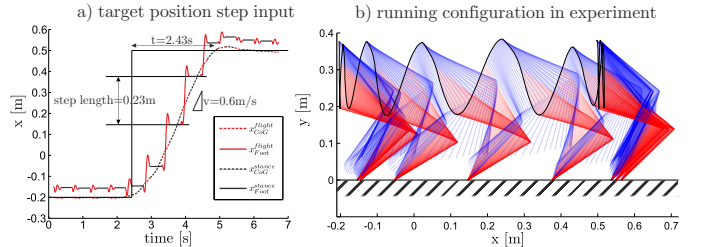


Fig. 13. 2D running experiments were successfully conducted with ScarlETH based on virtual model control.

($P_{rel} > 1$), and the motors can hence be reduced in size and weight. In both experiments, the joint springs lead to a large amplification of the output speed ($\omega_{rel} > 1$).

The controllability of ScarlETH is superior in comparison to FerrETH. Hopping height can be modified by changing the neutral point of the virtual spring element (12) while transition motions (e.g., from rest to hop or vice versa) or changes in the hopping frequency results from a very intuitive change of the virtual damping d_y , stiffness c_y parameters, or offset force g_y . The virtual forces in the horizontal direction (13) in combination with the angle of attack control (9) allows to reach arbitrary goal positions without any overshoot (Fig. 13), whereby step lengths of about 0.25m and top speeds of about 0.6m/s are achieved [25]. The mechanical cost of transport in this experiment with energy expenditure defined as the integral of positive mechanical motor power is about $COT = 0.9$, which is rather low in comparison with robotic devices of similar weight [21]. FerrETH is rather hard to control: changes in the desired hopping height always require a new adaptation of the hip motion profile [23], [34]. Reactions against uneven ground or other external disturbances are hence hard to achieve with this type of adaptive control.

VI. CONCLUSION

This paper summarizes the design and control of two robotic legs (FerrETH and ScarlETH) that were developed at our lab in order to combine *versatility*, *speed*, and *efficiency* in one single piece of hardware. We highlighted the various possibilities that these legs offer with respect to position/torque control as well as the exploitation of natural dynamic motions, and compared results for periodic hopping and running motions. Both legs are intended for integration in a quadruped robot that is able to robustly perform highly dynamic maneuvers and that shows large mobility in all joints. For the mechanical design, this enforced a very tight integration of all components (especially the springs), a lightweight construction with all actuators at the hip joint, and powerful motors.

Inspired by nature, where elastic elements in muscles and tendons largely contribute to an efficient running motion, we include large compliances in our system that not only protect the motors from impacts but also allow the temporary storage of energy. Internal collisions and nonlinear spring damper characteristics in the knee joint mechanically solve the damping dilemma: during the contact phase (when the joints are only deflected in one direction) very low mechanical damping ensures an efficient energy storage. As soon as the

leg leaves ground, it passes the neutral position which either leads to internal collisions (*FerrETH*) or to very high mechanical damping (*ScarETH*) and hence to a fast/immediate decrease of the undesired deflections. The two systems have one fundamental difference: In *FerrETH*, the hip joint remains position controlled based on high damping. This allows very accurate and fast joint position control while at the same time the motors are protected from impact loads. In contrast, the hip of *ScarETH* is built in a very compliant way that allows for precise torque control. Hand-in-hand design of the mechanical part and joint control facilitates active damping of the deflection oscillations during non-contact phases through a LQR control setup.

Although both systems demonstrated their applicability for planar running with similar performance with regard to system efficiency, *ScarETH* has a number of beneficial properties that favor it for future locomotion studies. The greatest advantage is its full torque controllability. In contrast to a complicated and restricted trajectory adaptation algorithm [23] that is necessary due to the missing precise torque controllability in the SDA hip joint, well studied and advanced (model based) torque control policies [33], [35], [36], [37] can be implemented. These very generic policies make the robot more versatile and robust, especially when it comes to complicated multi-legged systems. Hence, having with *ScarETH* a system that combines full torque and position control capability in one single device, this leg will be used in a quadruped running and climbing machine.

REFERENCES

- [1] G. A. Cavagna, N. C. Heglund, and C. R. Taylor, "Mechanical work in terrestrial locomotion: two basic mechanisms for minimizing energy expenditure," *AJP Regul Integr Comp Physiol*, vol. 233, no. 5, pp. 243–261, 1977.
- [2] M. H. Dickinson, C. T. Farley, R. J. Full, M. A. R. Koehl, R. Kram, and S. Lehman, "How animals move: An integrative view," *Science*, vol. 288, no. 5463, pp. 100–106, 2000.
- [3] K. Hirai, "Current and future perspective of honda humanoid robot," in *IEEE/RSJ International Conference on Intelligent Robots and Systems (IROS)*, 1997, pp. 500–508.
- [4] J. Yamaguchi, S. Inoue, D. Nishino, and A. Takanishi, "Development of a bipedal humanoid robot having antagonistic driven joints and three dof trunk," in *IEEE/RSJ International Conference on Intelligent Robots and Systems (IROS)*, 1998, pp. 96–101.
- [5] J. Estremera and P. Gonzalez de Santos, "Generating continuous free crab gaits for quadruped robots on irregular terrain," *IEEE Transactions on Robotics and Automation*, vol. 21, no. 6, pp. 1067–1076, 2005.
- [6] M. Kalakrishnan, J. Buchli, P. Pastor, M. Mistry, and S. Schaal, "Fast, robust quadruped locomotion over challenging terrain," in *IEEE International Conference on Robotics and Automation (ICRA)*, 2010.
- [7] K. Byl, K. Shkolnik, S. Prentice, N. Roy, and R. Tedrake, "Reliable dynamic motions for a stiff quadruped," *Experimental Robotics*, pp. 319–328, 2009.
- [8] C. D. Remy, O. Baur, M. Latta, A. Lauber, M. Hutter, M. H. Hoepflinger, C. Pradalier, and R. Siegwart, "Walking and crawling with alof: a robot for autonomous locomotion on four legs," *Industrial Robot: An International Journal*, vol. 38, no. 3, pp. 264–268, 2011.
- [9] M. H. Hoepflinger, C. D. Remy, M. Hutter, and R. Siegwart, "Haptic terrain classification on natural terrains for legged robots," in *International Conference on Climbing and Walking Robots (CLAWAR)*, 2010.
- [10] M. H. Raibert, *Legged robots that balance*, ser. The MIT Press series in artificial intelligence. Cambridge, Mass.: MIT Press, 1986.
- [11] R. M. Alexander, "3 uses for springs in legged locomotion," *International Journal of Robotics Research*, vol. 9, no. 2, pp. 53–61, 1990.
- [12] R. Blickhan, "The spring-mass model for running and hopping," *Journal of Biomechanics*, vol. 22, no. 11-12, pp. 1217–1227, 1989.
- [13] P. Gregorio, M. Ahmadi, and M. Buehler, "Experiments with an electrically actuated planar hopping robot," in *The 3rd International Symposium on Experimental Robotics III*. Springer-Verlag, 1994, pp. 269–281.
- [14] H. D. Taghirad, "Analysis, design, and control of hopping robot," 1993.
- [15] P. Gregorio, M. Ahmadi, and M. Buehler, "Design, control, and energetics of an electrically actuated legged robot," *IEEE Transactions on Systems Man and Cybernetics. Part B: Cybernetics*, vol. 27, no. 4, pp. 626–634, 1997.
- [16] L. R. Palmer, D. E. Orin, D. W. Marhefka, J. P. Schmideler, and K. J. Waldron, "Intelligent control of an experimental articulated leg for a galloping machine," in *IEEE International Conference on Robotics and Automation (ICRA)*, 2003, pp. 3821–3827.
- [17] H. De Man, D. Lefeber, and J. Vermeulen, *Design and Control of a Robot with One Articulated Leg for Locomotion on Irregular Terrain*. SpringerWienNewYork, 1998, vol. 405, ch. VI, pp. 417–424.
- [18] S. Curran and D. E. Orin, "Evolution of a jump in an articulated leg with series-elastic actuation," in *IEEE International Conference on Robotics and Automation (ICRA)*, 2008, pp. 252–258.
- [19] J. W. Hurst, "The role and implementation of compliance in legged locomotion," Ph.D. dissertation, 2008.
- [20] J. G. Nichol and K. J. Waldron, "Biomimetic leg design for untethered quadruped gallop," in *International Conference on Climbing and Walking Robots (CLAWAR)*, 2002.
- [21] A. D. Kuo, "Choosing your steps carefully: Trade-offs between economy and versatility in dynamic walking bipedal robots," *IEEE Robotics and Automation Magazine*, vol. 14, no. 2, pp. 18–29, 2007, 1070–9932.
- [22] M. Hutter, C. D. Remy, and R. Siegwart, "Design of an articulated robotic leg with nonlinear series elastic actuation," in *International Conference on Climbing and Walking Robots (CLAWAR)*, 2009.
- [23] ———, "Adaptive control strategies for open-loop dynamic hopping," in *IEEE/RSJ International Conference on Intelligent Robots and Systems (IROS)*, 2009.
- [24] M. Hutter, C. D. Remy, M. H. Hoepflinger, and R. Siegwart, "High compliant series elastic actuation for the robotic leg scarleth," in *International Conference on Climbing and Walking Robots (CLAWAR)*, 2011.
- [25] M. Hutter, C. D. Remy, M. H. Hoepflinger, and R. Y. Siegwart, "Scarleth: Design and control of a planar running robot," in *IEEE/RSJ International Conference on Intelligent Robots and Systems (IROS)*, 2011.
- [26] F. P. Boyle, N. K. Petek, and D. P. Smith, "Method for controlling motion using an adjustable damper," 2000.
- [27] J. E. Pratt and B. T. Krupp, "Series elastic actuators for legged robots," *Unmanned Ground Vehicle Technology Vi*, vol. 5422, pp. 135–144, 2004.
- [28] K. Kong, J. Bae, and M. Tomizuka, "A compact rotary series elastic actuator for human assistive systems," *IEEE/ASME Transactions on Mechatronics*, vol. 17, no. 2, pp. 288–297, 2012.
- [29] K. Kyoongchul, B. Joonbum, and M. Tomizuka, "Control of rotary series elastic actuator for ideal force-mode actuation in human and robot interaction applications," *IEEE/ASME Transactions on Mechatronics*, vol. 14, no. 1, pp. 105–118, 2009.
- [30] H. Vallery, R. Ekkelenkamp, H. van der Kooij, and M. Buss, "Passive and accurate torque control of series elastic actuators," in *IEEE/RSJ International Conference on Intelligent Robots and Systems (IROS)*, 2007, pp. 3534–3538.
- [31] C. D. Remy, K. W. Buffinton, and R. Y. Siegwart, "Energetics of passivity based running with high-compliance series elastic actuation," *International Journal of Mechatronics and Manufacturing Systems*, p. (accepted for publication), 2011.
- [32] C. D. Remy, K. W. Buffinton, and R. Siegwart, "A matlab framework for efficient gait creation," in *IEEE/RSJ International Conference on Intelligent Robots and Systems (IROS)*, 2011, pp. 190 – 196.
- [33] J. Pratt, C. M. Chew, A. Torres, P. Dilworth, and G. Pratt, "Virtual model control: An intuitive approach for bipedal locomotion," *International Journal of Robotics Research*, vol. 20, no. 2, pp. 129–143, 2001.
- [34] M. Hutter, "Hopping with an articulated robotic leg," ETH Zurich, Master Thesis, 2009.
- [35] L. Sentis, *Compliant Control of Whole-Body Multi-Contact Behaviors in Humanoid Robots*. Springer Global Editorial, 2009.
- [36] M. Mistry, J. Buchli, and S. Schaal, "Inverse dynamics control of floating base systems using orthogonal decomposition," in *IEEE International Conference on Robotics and Automation (ICRA)*, 2010, pp. 3406–3412.
- [37] M. Hutter, C. D. Remy, M. H. Hoepflinger, and R. Siegwart, "Slip running with an articulated robotic leg," in *IEEE/RSJ International Conference on Intelligent Robots and Systems (IROS)*, 2010.



Marco Hutter (1985) received the Master in Mechanical Engineering from the Swiss Federal Institute of Technology Zurich (ETHZ) in 2009. He is currently working toward a Ph.D. degree at the Autonomous System Lab at ETHZ. His research interest is dynamic locomotion with quadrupeds, whereby he is working on the hardware design, low level force and position control, as well as on model based walking and running using passive compliance.



C. David Remy is Assistant Professor of Mechanical Engineering at the University of Michigan. He holds a Masters in Mechanical Engineering from the University of Wisconsin at Madison, a Diploma in Engineering Cybernetics from the University of Stuttgart, and a Doctor of Science (PhD) from the Swiss Federal Institute of Technology (ETH) in Zurich. David Remys research interests include the design, simulation, and control of legged and other nonlinear systems. Drawing inspiration from biology and biomechanics, hes particularly interested in the effect and exploitation of natural dynamic motions, the role of different gaits, and the possibility of force/torque controllable systems; both in conceptual models and in hardware realization.



Mark A. Hoepflinger obtained his M.Sc. degree in Electrical Engineering and Information Technology from the Swiss Federal Institute of Technology (ETH Zurich) in 2007. He is currently working as a Ph.D student at the Autonomous Systems Lab, ETH Zurich. His main focus lies on research in the field of perception for walking robots.



Roland Siegwart (1959) is Full Professor for Autonomous Systems and Vice President Research and Corporate Relations at ETH Zurich since 2006 and 2010 respectively. After a Master and PhD in Mechanical Engineering at ETH Zurich, he was a postdoctoral fellow at Stanford University, senior researcher at ETH and R&D director at MECOS Traxler AG. From 1996 to 2006 he was Professor for autonomous robots at the EPFL Lausanne and member of the board of directors at the School of Engineering (2002-06). Roland Siegwart is a member of the Swiss Academy of Engineering Sciences, IEEE Fellow and officer of the International Federation of Robotics Research (IFRR). He served as Vice President (2004/05) and AdCom Member (2007/10) of the IEEE Robotics and Automation Society. He is and was coordinator of four European projects in the field of UAVs and autonomous robot navigation. Roland Siegwart was general chair of several conferences in robotics including IROS 2002, AIM 2007, FSR 2007, ISRR 2009 and is a co-founder of multiple successful spin-off companies in robotics.